MODEL AND CHARACTERISTIC OF A RESONANT TUNNELING NANOSTRUCTURE

MÔ HÌNH VÀ ĐẶC TÍNH CỦA MỘT CẤU TRÚC NANO ĐƯỜNG HẦM CỘNG HƯỞNG

Pham Thanh Trung
University of Technical Education —HCMC

Dinh Sy Hien,
University of Natural Sciences —HCMC

ABSTRACT:

This paper provides a brief tutorial for resonant tunneling theory and the operation of the future nanoelectronic devices using quantum effects employed in semiconductor industry for fabrication of computer devices and very high frequency oscillators. A typical model of resonant electronic transport through a double-barrier structure was developed. For each region of the system, analytic solutions to Schrödinger's equation were obtained, and these solutions formed the basis of the simulative code written to output plots of resonant peaks based on varying barrier parameters. Resonances in transmission probability and in the electron density inside the quantum well were then considered for a number of these different parameters. As an application of the model to device physics, a brief discussion of the concepts governing resonant tunneling devices is also included, especially prospects for applications in next generation optoelectronic nanostructures such as light emitting diodes, semiconductor quantum dot lasers.

Key words: *Resonant tunneling nanostructure, nanoelectronic device, quantum simulation*

TÓM TẮT:

Bài viết này đưa ra một bức tranh súc tích về lý thuyết hiệu ứng cộng hưởng đường hầm và hoạt động của các linh kiện điện tử nano dựa trên những hiệu ứng lượng tử trong công nghiệp bán dẫn dùng để chế tạo các linh kiện máy tính và bộ dao động siêu cao tần. Một mô hình đặc trưng truyền dẫn điện tử hiệu ứng cộng hưởng đường hầm thông qua cấu trúc hai rào đã được minh chứng. Trong mỗi vùng của hệ thống cấu trúc, phương trình Schrodinger lượng tử đã được phân tích với các đỉnh cộng hưởng phụ thuộc vào sự thay đổi thông số rào cản như đã chỉ ra trên công cụ mô phỏng. Sự cộng hưởng sẽ thay đổi tùy thuộc xác suất truyền và mật độ điện tử bên trong giếng thế với sự tác động của nhiều tham số khác nhau. Như một ứng dụng của mô hình vật lý linh kiện, một thảo luận vắn tắt về những triển vọng có thể ứng dụng cho những cấu trúc nano quang điện tử thế hệ mới như điốt phát sáng, laze chấm lượng tử bán dẫn.

Từ khóa: *Cấu trúc nano đường hầm cộng hưởng, linh kiện điện tử nano, mô phỏng lượng tử*

I. INTRODUCTION

The smaller the size of device is, the more difficult it is to fabricate, so the simulation will play an important role and be necessary for us to do experiments. During the past time, we focused on studying the physical models and analyzing the structural parameters of device for

the purpose of exact discussion of the concepts governing resonant tunneling structures (RTS). The basic quantum models have shown that analytic solutions to Schrödinger's equation were obtained, and that the quantum resonant tunneling formalism through a double-barrier structure was developed. Most of the presented researches in the world are derived from basic principles of the quantum tunneling formalism and contains parameters that originate from physical quantities. The physical nature of a nano-scopic model has only been considered for a number of these different parameters in a quantum system.

As an application of the model to device physics, we have contributed the interesting results for calculative model and experimental simulation on Matlab to output plots of the resonant peaks based on varying barrier-well parameters, temperature and composition of materials. In here our work, Matlab is probably the best one to model and simulate RTS's characteristics due to its easy use beside other tools. This is a useful and interesting study to help us to exactly understand the device's characteristics on very small size scales. These study agree very well with the results which were highly appreciated for experiments published in papers [1, 2, 3].

In this model we applied the quantum theory to solve the problem for the RTS with a double-barrier structure when we applied a bias voltage across the RTS. The effect of the bias voltage was analyzed specifically to illustrate the behavior of electrons tunneling through this structure. From the transmission probabilities for a number of different electron energies, we showed that current density is a function of incident energy. Then we calculated the total density of electrons inside the quantum well and the current through the two barriers.

II. QUANTUM THEORY MODELING

In order to introduce the concerning quantum model, we first consider the typical problem of a particle in a one dimensional (1-D) box. The behavior of the particle (electron) in this model follows from the solution of Schrödinger′s equation in one dimension, which gives rise to n discrete energy levels with n^2 spacing. As long as this idealistic box has infinite walls, the electron's wavefunction will be zero outside the box and purely sinusoidal inside and if this box is modified with walls of finite height, the particle has a chance to escape from or tunnel out of the confining potentials. High potentials relative to the energy of the particle and likewise, wide walls compared to the width of the well, correspond to less chance of escape, and hence a longer lifetime of the box's bound eigenstate.

And now, instead of picturing a particle sitting inside such a potential well, consider a coherent beam of electrons projected upon two such barriers of finite height and width, with the energy of the electrons lower than that of the barriers (see Fig. 1).

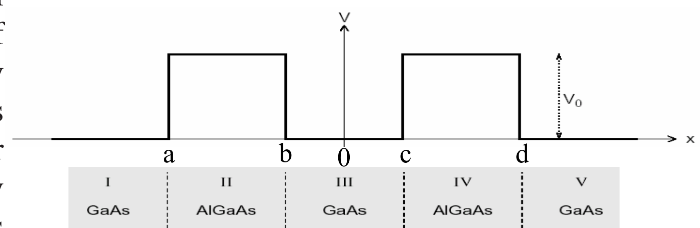

Fig. 1: Double barrier potential for resonant tunelling

In this 1-D model, when the incident flux encounters a potential barrier, it has only two options: reflection or transmission. The probability of transmission through the series of barriers peaks sharply at particular incident energies. The exact energy of these resonant modes depends on the height and width parameters describing the barriers and on the length of the well between them.

According to the modern quantum theory, the transmission coefficients themselves involves matching the solutions to the one-dimensional, time-independent Schrödinger equation in position space as the following:

$$\left[-\frac{\hbar^2}{2m}\frac{d^2}{dx^2}+V(x)\right]\psi(x)=E\psi(x) \qquad (1)$$

where m is the mass of the electron, and $\hbar = 1.055 \cdot 10^{-34}$ (J.s) in SI units [4].

We are assuming

a piecewise constant potential in this model.

$$\begin{cases} \dfrac{d^2\psi_1}{dx^2} + \dfrac{2m}{\hbar^2} E\psi_1 = 0 & \text{with} \quad x < a \\ \dfrac{d^2\psi_2}{dx^2} + \dfrac{2m}{\hbar^2}(E - V_0)\psi_2 = 0 & \text{with} \quad a \le x \le b \\ \dfrac{d^2\psi_3}{dx^2} + \dfrac{2m}{\hbar^2} E\psi_3 = 0 & \text{with} \quad b < x < c \\ \dfrac{d^2\psi_4}{dx^2} + \dfrac{2m}{\hbar^2}(E - V_0)\psi_4 = 0 & \text{with} \quad c \le x \le d \\ \dfrac{d^2\psi_5}{dx^2} + \dfrac{2m}{\hbar^2} E\psi_5 = 0 & \text{with} \quad x > d \end{cases} \tag{2}$$

where, $k_1 = \frac{1}{\hbar}\sqrt{2mE} = k_3 = k_5;\ k_2 = \frac{1}{\hbar}\sqrt{2m(E - V_0)} = k_4$

and assuming $E < V_0$ as is the case for the barriers here [4]. Considering all the regions of the given model and then solution of them as shown in (2),

$$\begin{cases} \psi_1 = Ae^{ik_1x} + Be^{-ik_1x} \\ \psi_2 = Ce^{ik_2x} + De^{-ik_2x} \\ \psi_3 = Fe^{ik_1x} + Ge^{-ik_1x} \\ \psi_4 = He^{ik_2x} + Ie^{-ik_2x} \\ \psi_5 = Je^{ik_1x} + Ke^{-ik_1x} \end{cases} \tag{3}$$

and beyond the barrier, which is the region x > d, particles may emerge moving in the positive x direction, so the wavefunction will have the form $\psi_5 = Je^{ik_1x}$ and in the region x < a, the wavefunction will have the form $\psi_1 = e^{ik_1x} + Be^{-ik_1x}$.

.

The last idea that we need to develop in order to calculate the transmission coefficients through series of barriers is that of probability current. We can briefly think of the probability of finding an electron in a particular spatial region changing due to a probability flow, or current, entering or leaving that region. This current we define as [5],

$$j_x = \frac{\hbar}{2mi}\left(\psi^* \frac{\partial\psi}{\partial x} - \psi\frac{\partial\psi^*}{\partial x}\right) \tag{4}$$

where $\psi^*(x)$ is the complex conjugate of $\psi(x)$

Finally, we define the transmission coefficient as $T = \frac{j_{trans,x>d}}{j_{inc,x<a}}$ [4].

The boundary conditions requiring both ψ and $\frac{d\psi}{dx}$ be continuous at x = a and x = b; x = c and x = d as

$$\begin{cases} \psi_1(a) = \psi_2(a); & \psi_2(b) = \psi_3(b) \\ \psi_3(c) = \psi_4(c); & \psi_4(d) = \psi_5(d) \end{cases}$$

and $$\left.\frac{d\psi_1}{dx}\right|_{x=a} = \left.\frac{d\psi_2}{dx}\right|_{x=a};\ \left.\frac{d\psi_2}{dx}\right|_{x=b} = \left.\frac{d\psi_3}{dx}\right|_{x=b};\ \left.\frac{d\psi_3}{dx}\right|_{x=c} = \left.\frac{d\psi_4}{dx}\right|_{x=c};\ \left.\frac{d\psi_4}{dx}\right|_{x=d} = \left.\frac{d\psi_5}{dx}\right|_{x=d} \tag{5}$$

then, we have

$$\begin{cases} e^{ik_1a} + Be^{-ik_1a} = Ce^{ik_1a} + De^{-ik_1a} \\ k_1e^{ik_1a} - k_1Be^{-ik_1a} = Ck_2e^{ik_2a} - k_2De^{-ik_2a} \\ Ce^{ik_2b} + De^{-ik_2b} = Fe^{ik_1b} + Ge^{-ik_1b} \\ k_2Ce^{ik_2b} - k_2De^{ik_2b} = k_1Fe^{ik_1b} - k_1Ge^{-ik_1b} \\ Fe^{ik_1c} + Ge^{-ik_1c} = He^{ik_2c} + Ie^{-ik_2c} \\ k_1Fe^{ik_1c} - k_1Ge^{ik_1c} = k_2He^{ik_2c} - k_2Ie^{-ik_2c} \\ He^{ik_2d} + Ie^{-ik_2d} = Je^{ik_1d} \\ k_2He^{ik_2d} - k_2Ie^{ik_2d} = k_1Je^{ik_1d} \end{cases} \qquad (6)$$

So, we match the boundary conditions at (5) and show that $\overline{\overline{M}}\,\overline{C} = \overline{A}$

where,

$$\overline{C} = \begin{pmatrix} B \\ C \\ D \\ F \\ G \\ H \\ I \\ J \end{pmatrix} \qquad \overline{A} = \begin{pmatrix} e^{-ik_1a} \\ k_1ae^{-k_1a} \\ 0 \\ 0 \\ 0 \\ 0 \\ 0 \\ 0 \end{pmatrix} \qquad (7)$$

$$\overline{\overline{M}} = \begin{pmatrix} -e^{-ik_1a} & e^{-ik_2a} & e^{ik_2a} & 0 & 0 & 0 & 0 & 0 \\ k_1e^{-ik_1a} & k_2e^{ik_2a} & -k_2e^{-ik_2a} & 0 & 0 & 0 & 0 & 0 \\ 0 & -e^{ik_2b} & -e^{-ik_2b} & e^{ik_1b} & e^{-ik_1b} & 0 & 0 & 0 \\ 0 & -k_2e^{ik_2b} & k_2e^{ik_2b} & k_1e^{ik_1b} & -k_1e^{-ik_1b} & 0 & 0 & 0 \\ 0 & 0 & 0 & -e^{ik_1c} & -e^{ik_1c} & e^{ik_2c} & e^{-ik_2c} & 0 \\ 0 & 0 & 0 & -k_1e^{ik_1c} & k_1e^{ik_1c} & k_2e^{ik_2c} & -k_2e^{-ik_2c} & 0 \\ 0 & 0 & 0 & 0 & 0 & -e^{ik_2d} & -e^{-ik_2d} & e^{ik_1d} \\ 0 & 0 & 0 & 0 & 0 & -k_2e^{ik_2d} & k_2e^{ik_2d} & k_1e^{ik_1d} \end{pmatrix} \qquad (8)$$

This problem can be solved for the coefficient vector C at (7) by $\overline{C} = \overline{\overline{M}}^{-1}\,\overline{A}$ (9)

The transmission coefficient is then

$$T = \left|\overline{C}(8)\right|^2 = |J|^2 \qquad (10)$$

and from $j_x = \frac{\hbar}{2mi}\left(\psi^* \frac{\partial \psi}{\partial x} - \psi \frac{\partial \psi^*}{\partial x}\right)$, we can calculate current density of transmission wave as $j_1 = j_T = |J|^2 \frac{\hbar k_1}{m}$ and the current flows through the device: $I_1 = j_1 \cdot S$ (11)

where S is the cross-sectional of the diode, specified in units of cm^2.

So far this form produces a peak current and a negative resistance, but there is no increasing valley current, which is due to tunneling through other channels and inelastic scattering. The simplest way to include a valley current contribution is to give it the form of tunneling through a higher resonance or thermal excitation over a barrier. For voltages below this higher energy channel, the additional current takes on the familiar diode form.

$$j_2 = j_s\left(e^{neV/kT} - 1\right) \text{ or } I_2 = I_s\left(e^{neV/kT} - 1\right) \qquad (12)$$

where j_s is the saturation current density, and I_s is is the saturation current [6].

Finally, the complete static current-voltage characteristic is the sum of the two current components at (11) and (12):

$$I = I_1 + I_2 = j_1 \cdot S + I_s\left(e^{neV/kT} - 1\right) \qquad (13)$$

The tunneling current's contribution to the total current is significant for a bias voltage across the RTS which has less value than a valley voltage, the excess current's contribution is significant for a bias voltage equal with a valley voltage is negligible and the contribution of the thermal current is significant for a bias voltage has more value than a valley voltage as shown in (13).

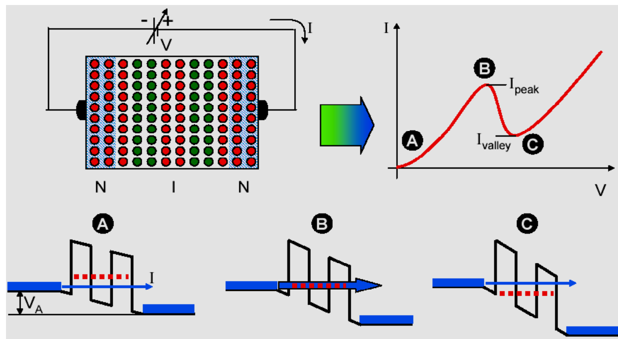

Fig.1: I-V characteristics and energy diagrams of resonant tunneling diode

Fig. 2: I-V characteristics and energy diagrams of a resonant tunneling structure

From the analysis above, we can predict the I-V characteristic for RTS as is shown in Fig. 2. As shown, because of the tunneling of electrons, current through RTS increases with the increase of V. Then when V continues to increase, after some point (I_{peak}), no electrons on the left can tunnel into the well, and current begins to decrease. If we keep increasing V, due to thermal mechanisms, current begins to increase once again.

In Fig.1, I_{peak} is the peak current generated by the tunneling of electrons. I_{valley} is the valley current due to the decrease in tunneling. Large ratio of I_{peak}/I_{valley} is desirable. This is because of the fact that large ratio means large gain for the negative differential resistor region. Secondly, large ratio often implies small I_{valley}. I_{valley} is usually the leakage current. So decreasing I_{valley} leads to decreasing power dissipation.

III. SIMULATIVE RESULTS

The following simulative results show that the transmission current depends not only on the quantum physical parameters but also on structural temperature and varying composition of materials. We combine the equations in (9), (10) and (13) to simulate the concerning structure. The illustration focuses primarily on explaining the I-V characteristics of RTS.

1. Temperature

The temperature plays an important role for the operation of the electronic devices on the integrated circuits. The larger the integrated density is, the much more the thermal energy generates. At room temperature I-V characteristic of AlGaAs/GaAs resonant tunneling structure exhibits a peak and a valley in the curve (this effect is sometimes referred to as

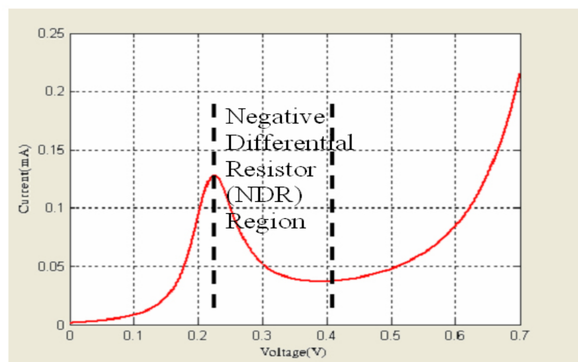

Fig. 3: The I-V characteristic at 300K (room temperature) with b= 6nm GaAs well and a=3nm AlGaAs barriers.

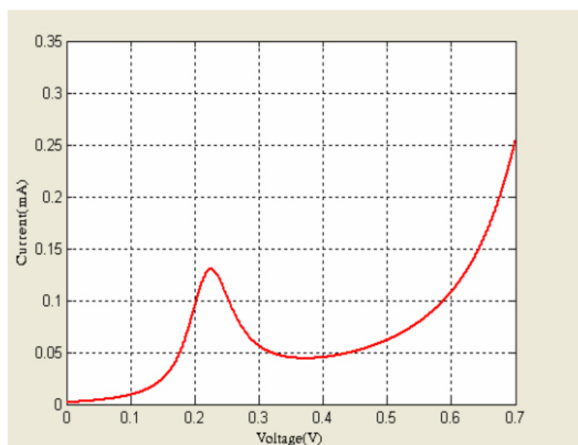

Fig. 4: The I-V characteristic at 400K with b=6nm GaAs well and a=3nm AlGaAs barriers.

Negative Differential Resistance (NDR) because of the way in which the resistance of the device decreases with increasing voltage in between the peak and the valley). Fig. 3 illustrates a peak current Ipeak = 0.13mA and a valley current Ivalley = 0.039mA, the PVR (high peak-to-valley ratio) = 3.4 (range 4:1 at room temperature) while at 400K, the PVR = 2.6 and at 800K, the PVR = 1.3. This means that the temperature of the device increases with decreasing the NDR and the

PVR.

Conversely, at low temperature the device operation is much better with a very high PVR. The devices work well and give a maximum PVR. The simulative results of the I-V characteristic show that device operation depends on the temperature, and current density is a function of temperature. Let's look at the different red curve from Fig. 3 to Fig. 6 at the different temperatures.

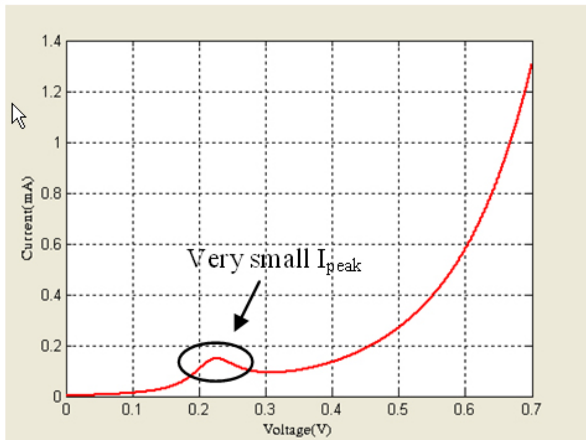

Fig. 5: The I-V characteristic at 800K with b=6nm GaAs well and a=3nm AlGaAs barriers.

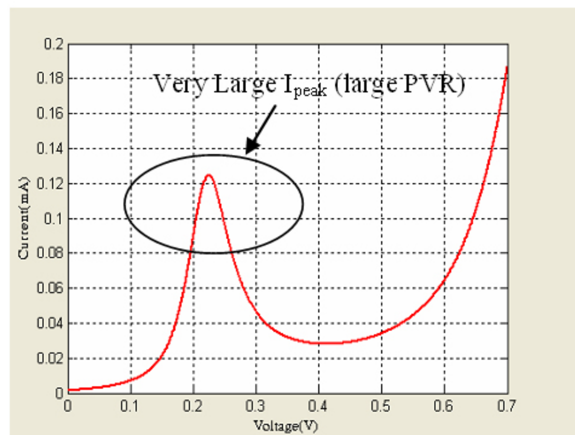

Fig .6: The I-V characteristic at 100K with b=6nm GaAs well and a=3nm AlGaAs barriers.

2. Quantum well-barrier width

In the double barrier structure, there is an extreme (exponential) sensitivity of the tunneling current to width of potential barriers [7]. This is also a difficulty intrinsic to the quantum mechanical tunneling effects employed in all the solid-state nanodevices. Its impact can only be mitigated by ensuring that all nanometer-scale barriers are made with extreme precision and uniformity in width. When the well width is larger, the I-V characteristic will turn out to be the I-V characteristic of the conventional diode. The one is changing the shape into the quantum well - barrier width as shown Fig. 7 to Fig. 8. The energy levels do not discontinue and quantum effects cannot be observed. Fig. 10 shows the characteristic curve with 500 nm barriers and 500 nm GaAs well is similar to the I-V characteristic of the conventional diode.

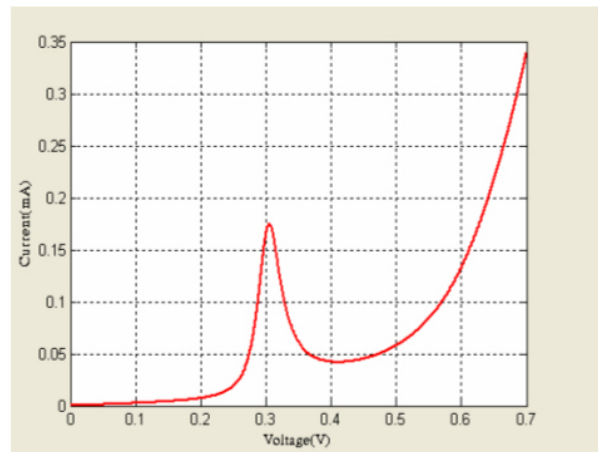

Fig. 7: The I-V characteristic at 300K with b=5nm GaAs well and a=5nm AlGaAs barriers.

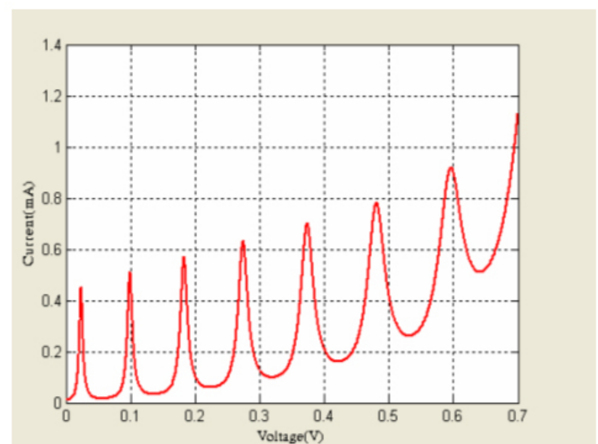

Fig. 8: The I-V characteristic at 300K with b=50nm GaAs well and a=3nm AlGaAs barriers.

The current-voltage characteristic at room temperature indicates not only that the major current-flow mechanism is convincingly tunneling in the reverse direction but also that tunneling may be responsible for current flow even in the low-voltage range of the forward direction.

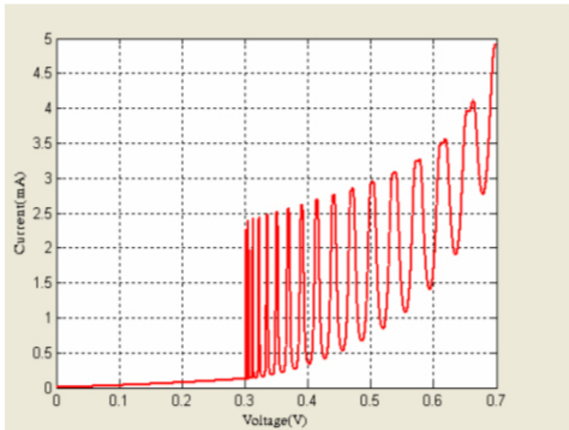

Fig. 9: The I-V characteristic at 300K with b=6nm GaAs well and a=100nm AlGaAs barriers.

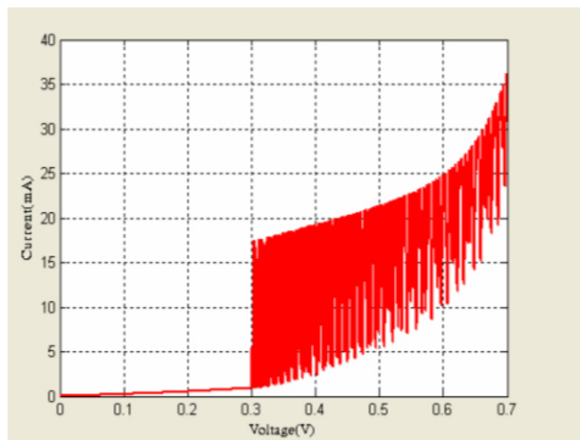

Fig. 10: The I-V characteristic at 300K with b=500nm GaAs well and a=500nm AlGaAs barriers.

By further narrowing the junction width (thereby further decreasing the tunneling path), through a further increase in the doping level, the negative resistance is clearly seen at all temperatures, as shown from Fig. 3 to Fig. 6.

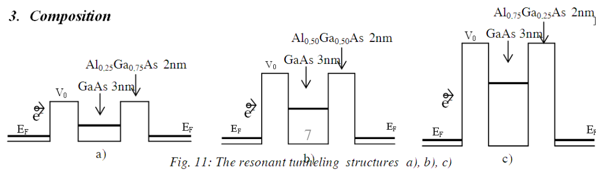

Fig. 11: The resonant tunneling structures a), b), c)

The effect of the composition of material on the I-V characteristic is very significant for device operation. The characteristic curve varied quickly with the Al mole fraction. Generally, in the basics of semiconductor heterostructures, a heterostructure is formed between any two dissimilar materials, examples of which are a metal and a semiconductor, an insulator and a semiconductor, or two different semiconductor materials. Semi-semiconductor heterostructures become increasing importance in electronic devices since they offer important new dimensions to device engineering. The formation of heterostructures, and the physical properties and aspects of heterostructures influence device behavior. Placing two dissimilar semiconductor materials into contact forms a semi-semiconductor heterostructure. Typically, a different semiconductor material is grown on top of another semiconductor using one of several epitaxial crystal growth techniques. Since the two constituent semiconductors within the heterostructure are of different types, many of their properties are distinctly different. The most important properties that influence the behavior of the heterostructure are the material lattice constants, energy gaps, doping concentrations, and affinity differences [8].

There are several different ways in which the energy bandgap discontinuity is accounted for at the interface. The type heterostructure is the most common that are sketched in Fig. 11 and a sketch of varying the Al composition in the AlGaAs barrier material can be seen from Fig. 12 to Fig. 14 respectively.

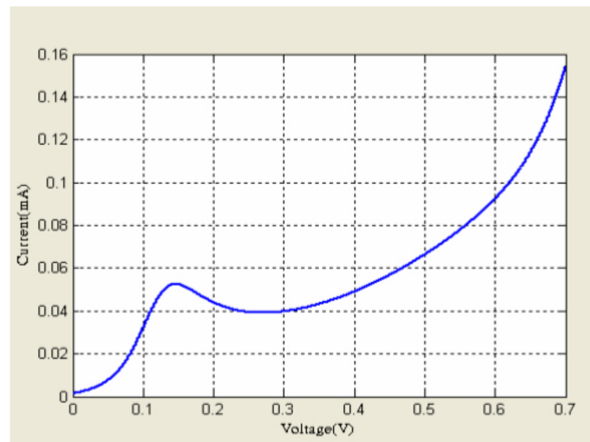

Fig.12: The I-V characteristic at room temperature with Al mole fraction x=0.25

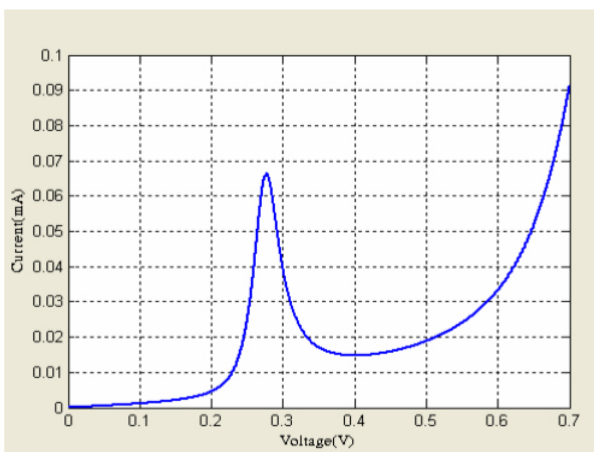

Fig.13: The I-V characteristic at room temperature with Al mole fraction x=0.5

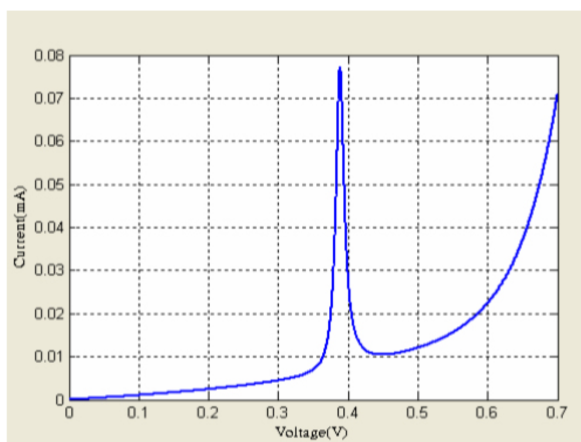

Fig.14: The I-V characteristic at room temperature with Al mole fraction x=0.75

IV. CONCLUSIONS

In summary, through the simulative tools our project leaded to the following important contributions. First, building the calculative model based on the quantum resonant tunneling theory to find out the I-V characteristics of the RTS. Second, device operation depending on varying the composition of material. Finally, a new material library including GaAs/AlGaAs, GaInAs/InP, GaInAs/AlInAs, GaSb/AlSb, GaN/AlN, InN/GaN was reported. For the different materials, effective electron mass is also an important element; a lower effective electron mass in the tunnel barrier will improve the NDR. It also improves the peak current density. A higher potential barrier improves the PVR, and a higher electron mobility gives a better operational frequency. Current density can be increased by making the barriers narrower, but beyond a certain point, the state bound in the well cannot be confined well enough, reducing the PVR. If we have a deep quantum well, resonance occurs through an excited state, which allows a higher current density (than through the ground state). Although the model we consider in this research comprises a number of significant physical simplifications, we have thoroughly understood it and have demonstrated numerically some general, known features of double-barrier tunneling, such as the behavior of the resonances. This model has demonstrated a number of interesting features and may be extended to any length series of quantum wells. It is useful to simulate the electrical behaviour of a device and very important for device design, especially prospects for applications in optoelectronic devices.

REFERENCES

[1] Sathya Sri Bandari, *Resonant Tunneling Devices (RTDs)*, ECE Dept. Rowan University, Glassboro NJ 08028.

[2] Sollner, T. C. L. G, "Resonant tunneling through quantum wells at frequencies up to 2.5 THz", *Applied Physics Letters 43*: 588 (1983).

[3] Leo Esaki, *Long journey into tunneling*, Nobel Lecture (1973).

[4] John S. Townsend, *A Modern Approach to Quantum Mechanics*, (University Science Books, Sausalito, CA, 2000), p. 147-188.

[5] David Bohm, *Quantum Theory*, Prentice-Hall, New York (1951).

[6] http://en.wikipedia.org/wiki/Diode

[7] Kevin F. Brennan, April S. Arown, *Theory of Modern Electronic Semiconductor Devices*. Georgia Institute of Technology, New York (2002).

[8] A. C. Seabaugh, J. H. Luscombe and Randall, "Quantum Functional Devices: Present Status and Future Prospects," *Future Electron Devices Journal*, Vol.3, p.9 - p.20 (1993).